LETTER

doi:10.1038/nature12722

Dysfunctional nitric oxide signalling increases risk of myocardial infarction

Jeanette Erdmann[1,2]*, Klaus Stark[3,4]*, Ulrike B. Esslinger[3,5]*, Philipp Moritz Rumpf[6,7]*, Doris Koesling[8], Cor de Wit[2,9], Frank J. Kaiser[2,10], Diana Braunholz[10], Anja Medack[1], Marcus Fischer[3], Martina E. Zimmermann[3], Stephanie Tennstedt[1], Elisabeth Graf[11,12], Sebastian Eck[11,12], Zouhair Aherrahrou[1,2], Janja Nahrstaedt[1], Christina Willenborg[1,2], Petra Bruse[1], Ingrid Brænne[1], Markus M. Nöthen[13,14], Per Hofmann[13,15], Peter S. Braund[16,17], Evanthia Mergia[8], Wibke Reinhard[6,7], Christof Burgdorf[6], Stefan Schreiber[18], Anthony J. Balmforth[19], Alistair S. Hall[20], Lars Bertram[21], Elisabeth Steinhagen-Thiessen[22], Shu-Chen Li[23,24], Winfried März[25,26,27], Muredach Reilly[28], Sekar Kathiresan[29,30,31], Ruth McPherson[32], Ulrich Walter[33,34], CARDIoGRAM†, Jurg Ott[35,36], Nilesh J. Samani[16,17], Tim M. Strom[11,12], Thomas Meitinger[6,11,12], Christian Hengstenberg[6,7] & Heribert Schunkert[6,7]

Myocardial infarction, a leading cause of death in the Western world[1], usually occurs when the fibrous cap overlying an atherosclerotic plaque in a coronary artery ruptures. The resulting exposure of blood to the atherosclerotic material then triggers thrombus formation, which occludes the artery[2]. The importance of genetic predisposition to coronary artery disease and myocardial infarction is best documented by the predictive value of a positive family history[3]. Next-generation sequencing in families with several affected individuals has revolutionized mutation identification[4]. Here we report the segregation of two private, heterozygous mutations in two functionally related genes, *GUCY1A3* (p.Leu163Phefs*24) and *CCT7* (p.Ser525Leu), in an extended myocardial infarction family. *GUCY1A3* encodes the α1 subunit of soluble guanylyl cyclase (α1-sGC)[5], and *CCT7* encodes CCTη, a member of the tailless complex polypeptide 1 ring complex[6], which, among other functions, stabilizes soluble guanylyl cyclase. After stimulation with nitric oxide, soluble guanylyl cyclase generates cGMP, which induces vasodilation and inhibits platelet activation[7]. We demonstrate *in vitro* that mutations in both *GUCY1A3* and *CCT7* severely reduce α1-sGC as well as β1-sGC protein content, and impair soluble guanylyl cyclase activity. Moreover, platelets from digenic mutation carriers contained less soluble guanylyl cyclase protein and consequently displayed reduced nitric-oxide-induced cGMP formation. Mice deficient in α1-sGC protein displayed accelerated thrombus formation in the microcirculation after local trauma. Starting with a severely affected family, we have identified a link between impaired soluble-guanylyl-cyclase-dependent nitric oxide signalling and myocardial infarction risk, possibly through accelerated thrombus formation. Reversing this defect may provide a new therapeutic target for reducing the risk of myocardial infarction.

The starting point of the present study (work flow in Supplementary Fig. 1) was the identification of a family with 32 members diagnosed with coronary artery disease (CAD), of whom 22 had early onset of the disease (≤60 years of age). Given the high mortality rates of myocardial infarction (MI), DNA was available from only 15 affected family members (Fig. 1 and Supplementary Fig. 2; clinical characteristics in Supplementary Table 1). Microsatellite-based linkage analysis failed to identify any significant single-locus log odds ratio (lod) scores. We decided to sequence the exome in three distantly related family members (III.13, III.24 and III.26; Fig. 1, for statistical and methodological considerations see Supplementary Information). Variants found in any of 800 control exomes from patients with unrelated diseases were excluded. Considering only rare, potentially functional relevant variants (minor allele frequency (MAF) $< 0.5\%$) and a dominant model, all three affected members showed two loss-of-function (*GUCY1A3* and *ETFDH*) and two non-synonymous (*CCT7* and *GCLC*) variants (Supplementary Table 2). These four variants were investigated (1) for presence in further control individuals, (2) for co-segregation pattern in the family assuming single- or two-locus linkage models (primers and PCR conditions in Supplementary Table 3), and (3) for biological links to CAD or MI in the literature (Supplementary Table 2). *ETFDH* and *GCLC* were not considered further, because neither single- nor two-locus linkage analysis produced a signal. Single-locus linkage analyses revealed a maximum lod score of 0.08 at recombination fraction $\theta_3 = 0.33$ for the variant in *GUCY1A3*, and 1.11 at $\theta_1 = 0.19$ in *CCT7*. However, in two-locus analyses, a maximum lod score of 5.68 was

[1]Institut für Integrative und Experimentelle Genomik, Universität zu Lübeck, 23562 Lübeck, Germany. [2]German Centre for Cardiovascular Research (DZHK), partner site Hamburg/Lübeck/Kiel, 23562 Lübeck, Germany. [3]Klinik und Poliklinik für Innere Medizin II, Universitätsklinikum Regensburg, 93053 Regensburg, Germany. [4]Department of Genetic Epidemiology, University of Regensburg, 93053 Regensburg, Germany. [5]Institut National de la Santé et de la Recherche Médicale (INSERM), UMR-S937 Paris, France. [6]Deutsches Herzzentrum München and 1. Medizinische Klinik, Klinikum rechts der Isar, Technische Universität München, 80636 München, Germany. [7]German Centre for Cardiovascular Research (DZHK), partner site Munich Heart Alliance, 80636 Munich, Germany. [8]Department of Pharmacology and Toxicology, Ruhr-University Bochum, 44801 Bochum, Germany. [9]Institut für Physiologie, Universität zu Lübeck, 23562 Lübeck, Germany. [10]Institut für Humangenetik, Universität zu Lübeck, 23562 Lübeck, Germany. [11]Institute of Human Genetics, Helmholtz Zentrum München, German Research Center for Environmental Health, 85764 Neuherberg, Germany. [12]Institute of Human Genetics, Technische Universität München, 81675 München, Germany. [13]Institute of Human Genetics, University of Bonn, 53127 Bonn, Germany. [14]Department of Genomics, Research Center Life & Brain, University of Bonn, 53127 Bonn, Germany. [15]Division of Medical Genetics, University Hospital Basel and Department of Biomedicine, University of Basel, 4003 Basel, Switzerland. [16]Department of Cardiovascular Sciences, University of Leicester, Leicester LE1 7RH, UK. [17]Leicester National Institute for Health Research Biomedical Research Unit in Cardiovascular Disease, Glenfield Hospital, Leicester LE1 7RH, UK. [18]Institute of Clinical Molecular Biology, Christian-Albrecht-Universität, 24105 Kiel, Germany. [19]Division of Cardiovascular and Diabetes Research, Multidisciplinary Cardiovascular Research Centre, Leeds Institute of Genetics, Health and Therapeutics, University of Leeds, Leeds LS2 9JT, UK. [20]Division of Cardiovascular and Neuronal Remodelling, Multidisciplinary Cardiovascular Research Centre, Leeds Institute of Genetics, Health and Therapeutics, University of Leeds, Leeds LS2 9JT, UK. [21]Department of Vertebrate Genomics, Max Planck Institute for Molecular Genetics, 14195 Berlin, Germany. [22]Charité Research Group on Geriatrics, Charité-Universitätsmedizin, 10117 Berlin, Germany. [23]Center for Lifespan Psychology, Max Planck Institute for Human Development, 14195 Berlin, Germany. [24]Department of Psychology, TU Dresden, 01062 Dresden, Germany. [25]Synlab Academy and Business Development, synlab Services GmbH, 68165 Mannheim, Germany. [26]Clinical Institute of Medical and Chemical Laboratory Diagnostics, Medical University of Graz, 8036 Graz, Austria. [27]Medical Clinic V, Medical Faculty Mannheim, University of Heidelberg, 68167 Mannheim, Germany. [28]The Cardiovascular Institute, University of Pennsylvania, Philadelphia, Pennsylvania 19104, USA. [29]Cardiovascular Research Center and Cardiology Division, Massachusetts General Hospital, Boston, Massachusetts 02215, USA. [30]Center for Human Genetic Research, Massachusetts General Hospital, Boston, Massachusetts 02215, USA. [31]Program in Medical and Population Genetics, Broad Institute of Harvard and Massachusetts Institute of Technology (MIT), Cambridge, Massachusetts 02215, USA. [32]University of Ottawa, Heart Institute, Ottawa, Ontario K1Y 4W7, Canada. [33]Centrum für Thrombose und Hämostase (CTH), Universitätsmedizin Mainz, 55131 Mainz, Germany. [34]German Centre for Cardiovascular Research (DZHK), partner site RheinMain, 55131 Mainz, Germany. [35]Institute of Psychology, Chinese Academy of Sciences, Beijing 100864, China. [36]Laboratory of Statistical Genetics, Rockefeller University, New York 10065, USA.

*These authors contributed equally to this work.

†A list of authors and their affiliations appears in the Supplementary Information.

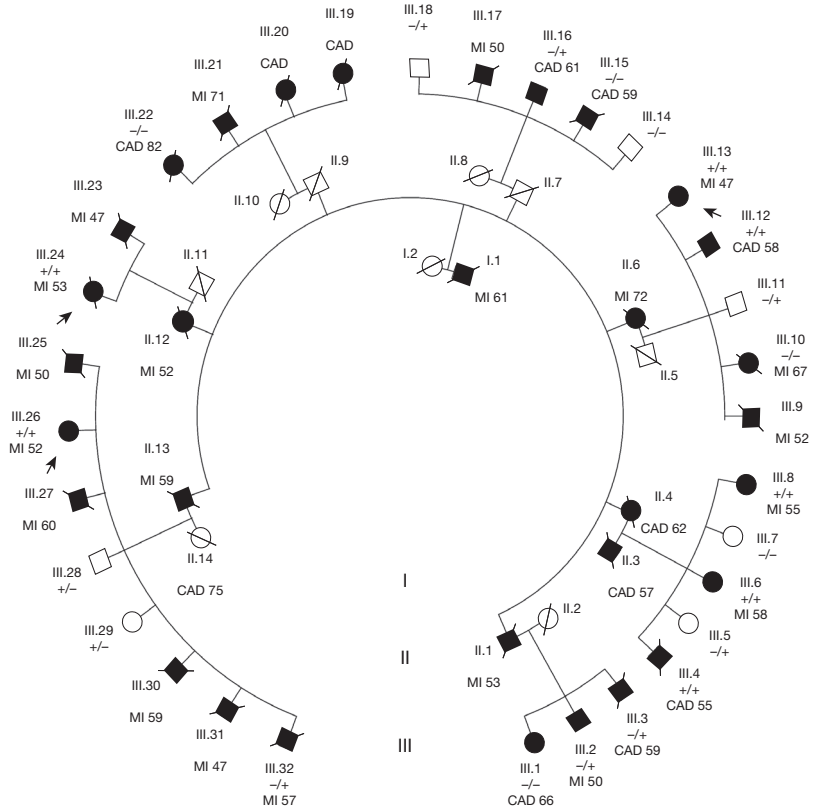

Figure 1 | Pedigree of the extended MI family with several individuals suffering from myocardial infarctions. White symbols denote healthy individuals, black symbols denote affected individuals; squares represent males, circles represent females. Crossed symbols represent deceased individuals. Age of onset is given next to the disease. MI, myocardial infarction; CAD, coronary artery disease. Persons III.13, III.24 and III.26 were exome-sequenced; +/+ denotes double-mutation carriers (p.Leu163Phefs*24^{+}/p.Ser525Leu^{-}); +/− denotes probands carrying only the p.Leu163Phefs*24 mutation in *GUCY1A3*; −/+ denotes probands carrying only the p.Ser525Leu mutation in *CCT7*.

obtained at $\theta_1 = 0.21$, with θ_2 fixed at 0.0001 (Supplementary Fig. 3 and Supplementary Information).

The single nucleotide insertion (T) in exon 6 of *GUCY1A3* (NM_001130683.2: c.488dup, p.Leu163Phefs*24) resulted in a frameshift and a premature stop codon after 24 aberrant amino acids. This variant was present in 7 out of 15 affected and 2 out of 7 unaffected family members for whom DNA was available. The second mutation is a single nucleotide substitution (C>T) in exon 10 of *CCT7* (NM_001166284) leading to a missense mutation at amino acid position 525 (p.Ser525Leu). It was present in 11 out of 15 affected and 3 out of 7 unaffected family members. Notably, all seven carriers of digenic mutations were affected (Fig. 1). Both mutations were absent in 3,150 healthy subjects and 3,842 unrelated MI cases, as determined by TaqMan technology, and are not listed in the current release of the NHLBI Exome Sequencing Project based on 6,503 samples drawn from multiple cohorts (Exome Variant Server, http://evs.gs.washington.edu/EVS/; accessed June 2013).

This finding of digenic inheritance underscores the importance of considering possible interactions between mutant proteins identified by sequencing experiments for understanding segregation patterns within families. It should be noted that some individuals in the family with single mutations had not developed the disease at the time of recruitment, and others had MI without carrying either mutation (Fig. 1). The latter can be expected, from a statistical point of view, for a highly prevalent disease and demonstrates a challenge in analysing the genetics of common conditions (Supplementary Information).

To study the linkage between rare *GUCY1A3* and *CCT7* variants and familial MI risk beyond this index family, the respective coding exons were sequenced (Supplementary Table 4) in 48 patients from 22 additional MI families with >5 affected family members (Supplementary Table 5), and p.Gly537Arg in *GUCY1A3* was identified in one affected family member. This highly conserved variant (Supplementary Fig. 4A) was subsequently found in 3 out of 5 affected members of this family, and was not present in the current 1000 Genome release[8], in the NHLBI Exome Sequencing Project (February 2013), or in 3,150 controls or 3,842 MI cases.

Furthermore, we searched for rare potential deleterious variants in *GUCY1A3* and *CCT7* in 252 young MI cases (age of onset between 24 and 49 years, 24% women) with a positive family history, and 800 individuals affected with other diseases (for example, mental retardation, type 2 diabetes, mitochondriopathy, Charcot–Marie–Tooth disease), for whom full exome sequencing data was available. In *GUCY1A3*, we identified 8 rare missense mutations (5 (2%) in CAD or MI, and 3 (0.37%) in other diseases, Fisher's exact test $P = 0.023$; Supplementary Table 6A). In *CCT7*, we identified 7 different missense mutations (3 (1.2%) in CAD or MI, and 5 (0.62%) in other diseases, $P = 0.12$; Supplementary Table 6B). Notably, p.Ser525Leu in *CCT7* was found in an additional patient suffering from premature MI (age of onset 43 years). No other person carrying mutations in both *GUCY1A3* and *CCT7* genes was found.

We analysed the functional implications of the two newly identified rare variants in *GUCY1A3* (p.Leu163Phefs*24 and p.Gly537Arg), which encodes the α1 subunit of soluble guanylyl cyclase (α1-sGC), by introducing respective point mutations and transfection into human embryonic kidney 293 (HEK 293) cells (Fig. 2). Compared to transfection using a wild-type transgene, the amount of α1-sGC protein was reduced by 96% (p.Leu163Phefs*24) and 80% (p.Gly537Arg) after mutant transfection. This was associated with an almost complete loss of enzyme activity in cells transfected with these mutants (<10% of wild-type cGMP production after nitric oxide (NO) stimulation). The reduced protein content of the p.Gly537Arg mutant is probably due to impaired stability of the mutated protein.

To evaluate the relevance of CCTη for sGC protein integrity, the protein was successfully reduced by short interfering RNA (siRNA) in human aortic smooth muscle cells (HASMC) with three pooled *CCT7*-specific siRNAs (10–20 nM), but remained unchanged in controls (scrambled siRNA), as verified by western blot. Downregulation of CCTη markedly decreased protein levels of the α1 and β1 subunits

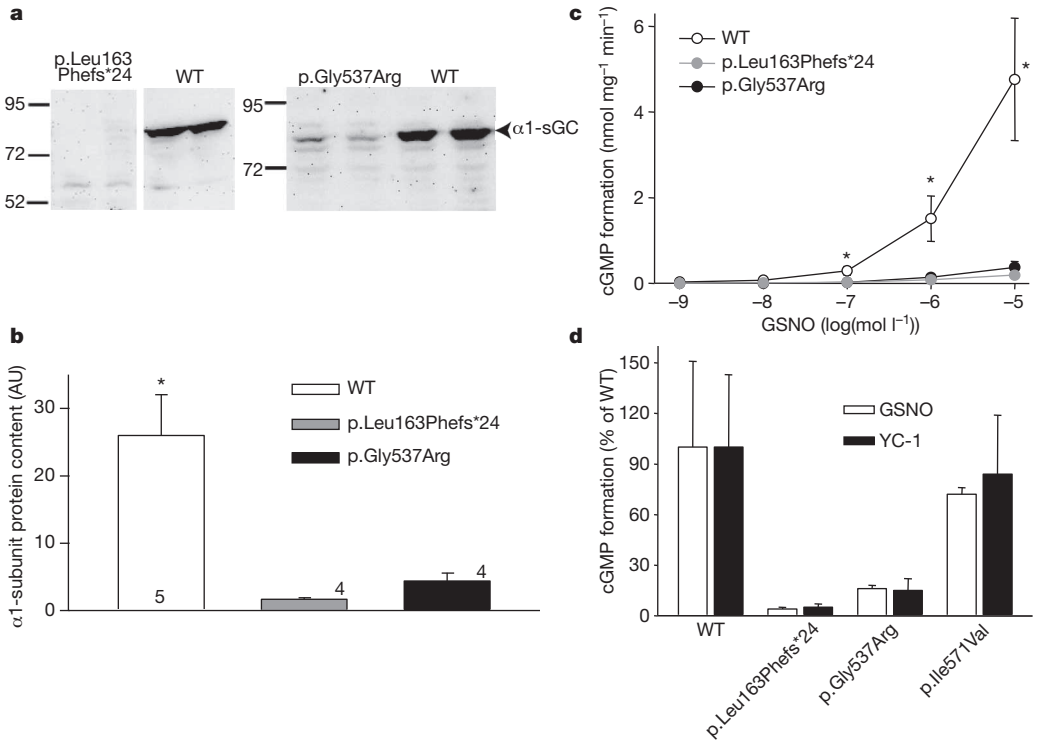

Figure 2 | Reduced expression and enzymatic activity of the identified sGC mutants in HEK 293 cells. **a**, **b**, *GUCY1A3* mutants were expressed together with β1-sGC in HEK 293 cells. Representative western blots of α1-sGC expression are shown (**a**); α1-sGC protein was strongly reduced in mutants (**b**, numbers in bars are independent transfections performed in duplicates). **c**, Accordingly, NO-induced concentration-dependent cGMP formation was significantly attenuated after transfection with mutant proteins ($n = 7$ (wild type; WT) or 4 experiments). **d**, cGMP formation was similarly reduced if sGC was activated by a pharmacological stimulator (YC-1, 100 μM; $n = 3$). GSNO, *S*-nitrosoglutathione; YC-1, 3-(5′-hydroxymethyl-2′-furyl)-1-benzylindazole. $^*P < 0.05$ versus other groups (Mann–Whitney, Bonferroni corrected). AU, arbitrary units. Error bars indicate s.e.m.

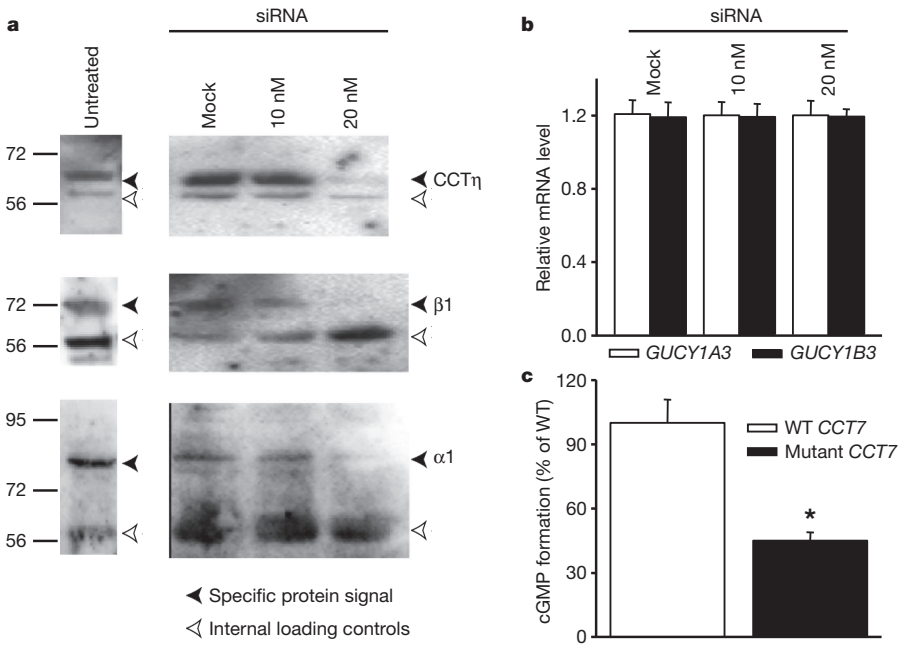

Figure 3 | CCTη is required for sGC expression and function. **a**, Expression of CCT7 was downregulated by transfection of 20 nM *CCT7* siRNAs in HASMC, but unchanged by scrambled (mock, 20 nM) or 10 nM *CCT7* siRNA compared to extracts of untreated HASMC. Reduction of *CCT7* decreased β1-sGC protein levels, and α1-sGC was correspondingly reduced (representative for six experiments). **b**, Quantitative PCR analyses excluded alterations on *GUCY1A3* (α1) and *GUCY1B3* (β1) mRNA levels by siRNA-mediated decrease of CCTη. **c**, NO-stimulated cGMP formation was strongly reduced in HEK 293 cells co-transfected with sGC (α1β1) and mutated CCTη (p.Ser525Leu) compared to wild-type CCTη. $n = 4$, $^*P < 0.05$ versus wild type (paired *t*-test). Error bars indicate s.e.m.

of sGC, whereas the sGC subunits were unaffected in controls (Fig. 3a). However, messenger RNA levels of *GUCY1A3* (α1) and *GUCY1B3* (β1) were not affected by siRNA-mediated *CCT7* knockdown (Fig. 3b). These data identify a functional role for CCTη in maintaining sGC protein levels, presumably by stabilizing the sGC protein complex. The functional effect of the identified mutation in *CCT7* was studied by co-expression of mutant (p.Ser525Leu) or wild-type *CCT7*, together with α1- and β1-sGC in HEK 293 cells. Analysis of NO-stimulated cGMP formation revealed reduced sGC activity (by ~50%) in cells expressing mutant compared to wild-type *CCT7* (Fig. 3c).

We then measured sGC protein and cGMP-forming activity in isolated platelets from family members. Three affected digenic mutation carriers, five mutation carriers with either *GUCY1A3* (p.Leu163Phefs*24) or *CCT7* (p.Ser525Leu) mutation, and four non-carriers were available for this study. Platelets of digenic mutation carriers contained significantly less α1- and β1-sGC, and also produced significantly lower amounts of cGMP after stimulation with NO compared to single-mutation carriers or non-carriers (Fig. 4).

cGMP formation in individuals carrying only the *GUCY1A3* p.Leu163Phefs*24 variant was lower than in non-carriers (2.0 ± 0.0 nmol mg^{-1} min^{-1} versus 3.1 ± 0.4 nmol mg^{-1} min^{-1}). Yet, as only two individuals with just the *GUCY1A3* p.Leu163Phefs*24 variant were available for these measurements, this observation is not statistically significant. cGMP formation in platelets of mice heterozygous for α1-sGC was reduced by roughly 50%, clearly demonstrating that both gene copies contribute to sGC function in mice (Supplementary Fig. 6).

Platelet aggregation represents an important feature of thrombus formation in MI. Several pathways stimulate platelet aggregation, and cGMP inhibits platelet activation[9]. Having observed the effect of *GUCY1A3* and *CCT7* mutations on sGC expression and cGMP production, we directly tested the effect of a loss of *GUCY1A3 in vivo*, and demonstrated that mice lacking α1-sGC had enhanced thrombus formation (Fig. 5), providing a potential mechanistic link between the identified mutations in the sGC pathway and MI through an enhanced thrombotic tendency.

Notably, two recent large-scale genome-wide association studies (GWAS)[10,11] identified a common variant (rs769238) on chromosome 4q32.1 overlapping with the *GUCY1A3* gene, and this variant displayed genome-wide significant association with CAD or MI (the risk allele frequency of rs7692387 is about 80%) (Supplementary Fig. 7a, b). As with any significant GWAS hit, this only indicates a suggestion that the nearby gene is involved. However, our findings of rare variants in two families and in unrelated MI and CAD cases, as well as the *in vitro*/*in vivo* experimental data, now provide substantial evidence for the

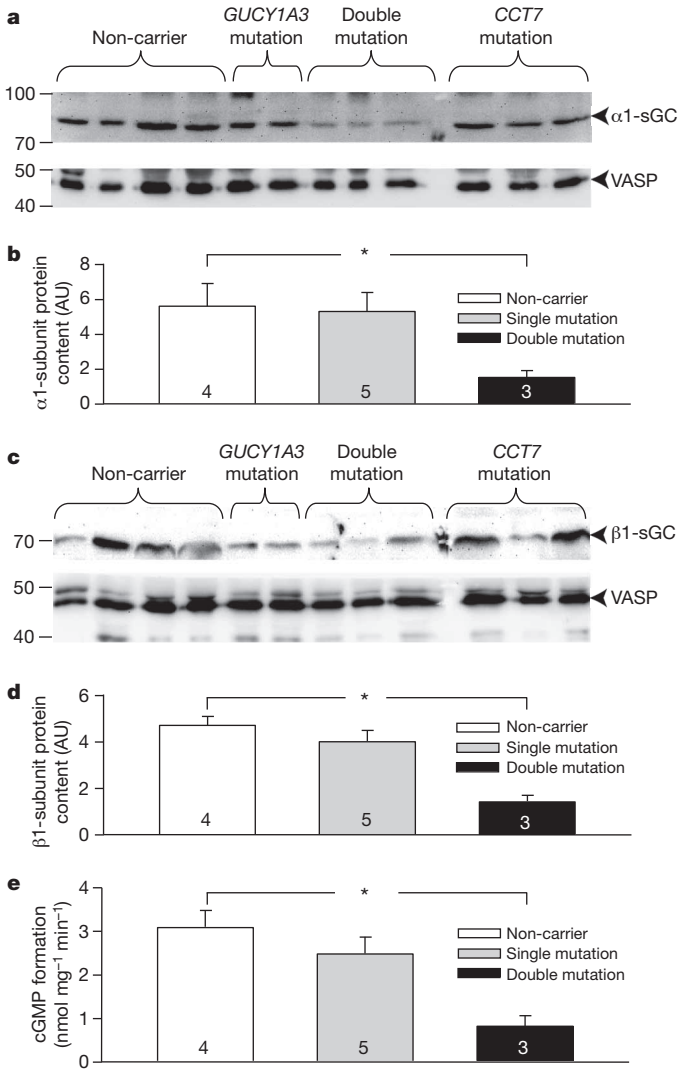

Figure 4 | Reduced sGC expression and activity in platelets of double-mutation carriers. a–d, Expression of α1- and β1-sGC in platelets of members from family 2001 is shown by representative western blot (**a**, **c**) and quantified in quadruplicates (**b**, **d**) (loading control: VASP). Single-mutation carriers are merged in a single group because western blotting did not reveal obvious differences between them. **e**, Only double-mutation carriers exhibited reduced amounts of α1-sGC and attenuated NO-dependent cGMP formation (100 μM GSNO), determined in homogenates of platelets. The dimerizing partner, β1-sGC, was reduced accordingly in double-mutation carriers (**c**, **d**). Numbers in bars denote the number of family members analysed. *$P < 0.05$ (*t*-test, only non-carriers). Error bars indicate s.e.m.

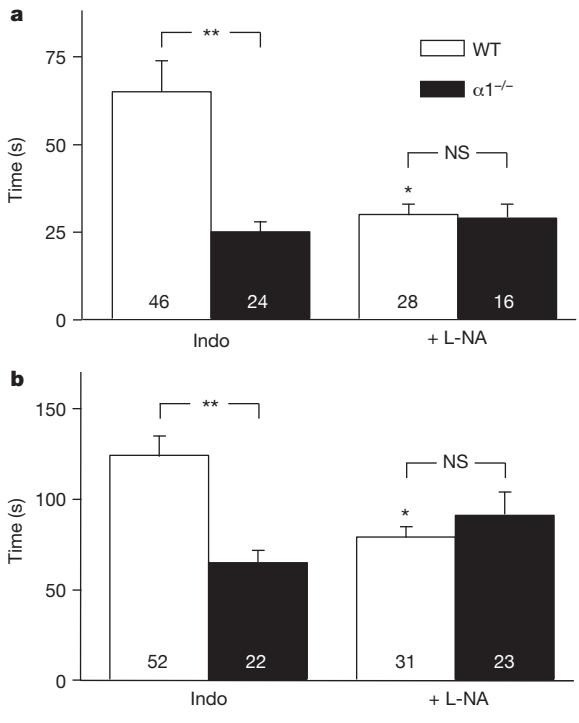

Figure 5 | Thrombus formation in-vivo in mice deficient for the α1-sGC (α1$^{-/-}$). Thrombus formation was initiated in arterioles by photoexcitation. **a**, **b**, Time to visible thrombus formation (**a**) and complete occlusion (**b**) indicated by flow stop were assessed during prostaglandin inhibition (indometacin (indo), 3 μM) and after additional NO synthase inhibition (*N*-nitro-L-arginine (L-NA), 30 μM). Thrombus formation was accelerated in α1$^{-/-}$ mice after indometacin. Inhibition of NO enhanced thrombus formation only in wild type, and abolished differences between genotypes, indicating that endogenous NO counteracts thrombus formation in wild-type, but not in α1$^{-/-}$ mice. Numbers in bars indicate numbers of arterioles studied in 7 α1$^{-/-}$ and 14 wild-type mice. *$P < 0.05$ versus indometacin; **$P < 0.01$ between genotypes (Mann–Whitney). Error bars indicate s.e.m.

causal involvement of guanylyl cyclase variation in the disease process studied in the GWAS[10,11].

One objective of identifying pathways associated with disease risk is to find new therapeutic targets. Further confirmation is required whether variants in *GUCY1A3* and *CCT7* affect MI risk through platelet activation or other mechanisms. Nevertheless, the sGC system is particularly amenable to therapy and a new class of cardiovascular drugs, for example, sGC stimulators or activators, are increasingly recognized as a treatment option for cardiovascular diseases[12]. Our genetic and functional findings provide strong support for further pursuit of this possibility in relation to MI. Furthermore, our study highlights the challenges and opportunities of large-scale sequencing in severely affected families, as novel disease mechanisms (impaired sGC activity causing MI), unexpected contributors to the molecular aetiology (a chaperone), and unusual inheritance patterns (synergistic digenic mutations) may come together and explain a rather private disease entity.

METHODS SUMMARY

Exome sequencing in three affected cousins of a large MI family was performed on a Genome Analyzer IIx system (Illumina). Linkage analysis was carried out using the Affymetrix Human Mapping 10K Array. We assumed a high-penetrance general dominant model and constructed a multiplicative (interaction, epistasis), two-locus model using the LINKAGE (single-locus models) and TLINKAGE (two-locus models) programs. The functional implications of the rare variants were analysed by introducing respective point mutations in α1-sGC encoded by *GUCY1A3* and co-expression with β1-sGC in HEK 293 cells. To evaluate the functional relevance of CCTη, *CCT7* expression was reduced by siRNA in HASMC. The effect of CCTη mutation was assessed by measuring sGC activity in HEK 293 cells co-expressing sGC and mutant or wild-type CCTη. cGMP-forming activity was measured in isolated platelets from family members and mice heterozygous for α1-sGC. We monitored arteriolar thrombus formation in mice deficient for α1-sGC in response to a confined focused trauma (photoexcitation) in the microcirculation *in vivo*.

Online Content Any additional Methods, Extended Data display items and Source Data are available in the online version of the paper; references unique to these sections appear only in the online paper.

Received 22 March 2012; accepted 27 September 2013.
Published online 10 November 2013.

1. World Health Organization. The top 10 causes of death. Fact sheet no. 310; http://www.who.int/mediacentre/factsheets/fs310/en/index.html (2011).
2. Finn, A. V., Nakano, M., Narula, J., Kolodgie, F. D. & Virmani, R. Concept of vulnerable/unstable plaque. *Arterioscler. Thromb. Vasc. Biol.* **30,** 1282–1292 (2010).
3. Lloyd-Jones, D. M. *et al.* Parental cardiovascular disease as a risk factor for cardiovascular disease in middle-aged adults: a prospective study of parents and offspring. *J. Am. Med. Assoc.* **291,** 2204–2211 (2004).
4. Bamshad, M. J. *et al.* Exome sequencing as a tool for Mendelian disease gene discovery. *Nature Rev. Genet.* **12,** 745–755 (2011).
5. Mergia, E., Friebe, A., Dangel, O., Russwurm, M. & Koesling, D. Spare guanylyl cyclase NO receptors ensure high NO sensitivity in the vascular system. *J. Clin. Invest.* **116,** 1731–1737 (2006).
6. Leitner, A. *et al.* The molecular architecture of the eukaryotic chaperonin TRiC/CCT. *Structure* **20,** 814–825 (2012).
7. Zabel, U., Weeger, M., La, M. & Schmidt, H. H. Human soluble guanylate cyclase: functional expression and revised isoenzyme family. *Biochem. J.* **335,** 51–57 (1998).
8. The 1000 Genomes Project Consortium. A map of human genome variation from population-scale sequencing. *Nature* **467,** 1061–1073 (2010).
9. Moro, M. A. *et al.* cGMP mediates the vascular and platelet actions of nitric oxide: confirmation using an inhibitor of the soluble guanylyl cyclase. *Proc. Natl Acad. Sci. USA* **93,** 1480–1485 (1996).
10. Deloukas, P. *et al.* Large-scale association analysis identifies new risk loci for coronary artery disease. *Nature Genet.* **45,** 25–33 (2013).
11. Lu, X. *et al.* Genome-wide association study in Han Chinese identifies four new susceptibility loci for coronary artery disease. *Nature Genet.* **44,** 890–894 (2012).
12. Stasch, J. P., Pacher, P. & Evgenov, O. V. Soluble guanylate cyclase as an emerging therapeutic target in cardiopulmonary disease. *Circulation* **123,** 2263–2273 (2011).

Supplementary Information is available in the online version of the paper.

Acknowledgements We thank all the family members who participated in this research. Without the continuous support of these patients over more than 15 years, the present work would not have been possible. We would like to thank S. Wrobel, S. Stark, A. Liebers, K. Franke, J. Stegmann-Frehse, M. Behrensen, M. Schmid, J. Eckhold, D. Wöllner, U. Krabbe and J. Simon for technical assistance. Furthermore, we would like to thank M. Becker, N. Buchholz, I. Demuth, R. Eckardt, H. Heekeren, U. Lindenberger, M. Lövdén, L. Müller, W. Nietfeld, G. Pawelec, F. Schmiedeck, T. Siedler and G. G. Wagner for their contributions to BASE-II. We also would like to thank S. Herterich and S. Gambaryan for advice, and B. Mayer, U. Hubauer, K.-H. Ameln and A. Großhennig for help with GerMIFS. We thank WTCCC+ and the WTCCC-CAD2 investigators for access to their data. The study is supported by the Deutsche Forschungsgemeinschaft and the German Federal Ministry of Education and Research (BMBF) in the context of the German National Genome Research Network (NGFN-2 (01GS0417) and NGFN-plus (01GS0832)), the FP6 and FP7 EU-funded integrated projects Cardiogenics (LSHM-CT-2006-037593), ENGAGE (201413), and GEUVADIS (261123), the binational BMBF/ANR funded project CARDomics (01KU0908A), the local focus programs 'Kardiovaskuläre Genomforschung' and 'Medizinische Genetik' of the Universität zu Lübeck, and the University Hospital of Regensburg, Germany. The German Federal Ministry for Education and Research provided funding for BASE-II (BMBF; grant no. 16SV5538). Support by NSFC grant 30730057 from the Chinese Government (to J.O.) is gratefully acknowledged. N.J.S. holds a Chair funded by the British Heart Foundation, and is supported by the Leicester NIHR Biomedical Research Unit in Cardiovascular Disease. U.W. is supported by the BMBF (01EO1003). M.M.N. is a member of the DFG-funded Excellence Cluster ImmunoSensation.

Author Contributions J.E., C.H., F.J.K., T.M., N.J.S., H.S. and K.S. designed the study. Z.A., D.B., P.B., C.d.W., S.E., U.B.E., E.G., F.J.K., D.K., A.M., E.M., W.R., P.M.R., T.M.S. and M.E.Z. conducted the experiments. I.B., M.F., J.N., J.O., K.S., T.M.S., S.T. and C.W. analysed the data. A.J.B., L.B., P.S.B., C.B., A.S.H., P.H., S.K., S.-C.L., W.M., R.M., T.M., M.M.N., M.R., N.J.S., S.S., E.S.-T. and U.W. provided material, data and analysis tools. J.E., C.d.W., C.H., F.J.K., N.J.S. and H.S. wrote the paper. C.H. and H.S. contributed equally. See Supplementary Information for Members of CARDIoGRAM.

Author Information Variant data is available in ClinVar (http://www.ncbi.nlm.nih.gov/clinvar/) with accession numbers SCV000083870 for NM_001130683.2:c.488dup and SCV000083871 for NM_001166284.1:c.1313C>T. Reprints and permissions information is available at www.nature.com/reprints. The authors declare no competing financial interests. Readers are welcome to comment on the online version of the paper. Correspondence and requests for materials should be addressed to C.H. (hengstenberg@dhm.mhn.de) or J.E. (jeanette.erdmann@iieg.uni-luebeck.de).

METHODS

Extended MI families and unrelated samples. The ascertainment strategy of MI families is described elsewhere[13,14] and in the Supplementary Information. In brief, index patients had suffered from MI before the age of 60 years. If at least one additional living sibling presented with MI or severe CAD (defined by percutaneous coronary intervention or coronary artery bypass grafting), the entire family (index patient, available parents and all siblings) was contacted and invited to participate in the study. A total of 26 extended families could be recruited, each with more than 5 living CAD or MI patients, and totalling $n = 1{,}001$ individuals. Figure 1 depicts the pedigree of the MI family used for exome sequencing. Clinical and angiographic characteristics are detailed in Supplementary Table 1.

Exome sequencing. Exome sequencing was performed as 54-bp (base pair) paired-end runs on a Genome Analyzer IIx system (Illumina) after in-solution enrichment of exonic sequences (SureSelect Human All Exon 38 Mb kit, Agilent), yielding on average 6.2 gigabases (Gb) of sequence per individual. The average read depth was 78, with between 84.5 and 85.6% of the target regions covered at least 20×. Read alignment was performed with BWA (v. 0.5.8) using the default parameters. We used the human genome assembly hg19 (GRCh37) as reference. A small percentage of duplicate reads (4–5%) were removed. Single nucleotide variants (SNVs) and small insertions and deletions (indels) were detected using SAMtools (v 0.1.7). For the variant filter part of SAMtools, we used the default parameters with the exception of setting a maximum read depth to 9,999. Furthermore, we required putative SNVs to fulfil the following criteria: (1) median base quality of the variant bases of at least 15; (2) a minimum of 15% of reads showing the variant base; and (3) the variant base is indicated by at least 5% of reads coming from different strands. Variant annotation was performed using custom Perl scripts, using data from dbSNP (v131) and the UCSC Genome Browser 'knownGene' track.

Mutation validation. Annotations of SNVs were based on the UCSC database. Mutation validation was performed through PCR and Sanger sequencing of candidate gene region identified via exome sequencing. After confirmation of variants, additional family members were screened considering co-segregation. Primers used for mutation validation and PCR conditions are listed in Supplementary Table 3. We sequenced the coding exons (Supplementary Table 4) of the 2 genes in 48 patients from 22 additional MI families with >5 affected family members (Supplementary Table 5). PolyPhen-2 prediction was done for all non-synonymous SNVs (http://genetics.bwh.harvard.edu/pph2/)[15].

Linkage analysis. Linkage analysis was carried out using the Affymetrix Human Mapping 10K Array. For the genetic linkage analysis, we assumed a high-penetrance general dominant model (for details see Supplementary Table 7). Taking these penetrances as marginal penetrances for each of two loci, we constructed a multiplicative (interaction, epistasis) two-locus model[16]. Analyses were carried out with the Windows versions of the LINKAGE (single-locus models) and TLINKAGE (two-locus models) programs.

For two-locus analysis, we assumed the locus order M_1–D_1–D_2–M_2, in which M refers to marker loci and D to disease loci. Recombination fractions in the three intervals are denoted by θ_1, θ_2 and θ_3, for M_1–D_1, D_1–D_2 and D_2–M_2, respectively. Initially, all three recombination fractions were estimated iteratively, resulting in values of 0.210, 0 and 0.436, respectively. As the two disease loci appeared closely linked, we assumed a fixed recombination fraction of $\theta_2 = 0.0001$ between them, which furnished estimates of $\theta_1 = 0.216$ and $\theta_3 = 0.5$. As marker M_2 appeared essentially unlinked with the other loci, we focused on marker M_1 and its relation with the two-locus cluster D_1–D_2.

Homology modelling. For human CCTη, several homologue X-ray structures are available. We used the yeast T-complex protein 1 subunit η (TCP1-η) as template (PDB accession 3P9G, chain G[17]) for the homology model of human CCTη. The template was received by blast search and allowed us to calculate a human CCTη model containing the amino acid p.Ser525Leu. The model was built with the YASARA 10.8.16 software package by default settings[18]. In this study, we used the hybrid model of 20 generated initial models. The model was energy-minimized by YAMBER3 force field[19,20] to remove bumps and correct the covalent geometry. After removal of conformational stress by a short steep descent minimization, the procedure continued by simulated annealing until convergence was reached. The average quality Z-score after validation with WHAT_CHECK was −1.5. This means that the model is 1.5 standard deviations below average and can be considered as good. For none of the GTP sGCs, NMR data or X-ray structures are available. Therefore, we have built a homology model of human sGC using the theoretical three-dimensional structure of bovine sGC in complex with GTP[21] (PDB accession 1AWN). The resulting model comprises the amino acids p.V472 to p.L627 of *GUCY1A3* in complex with *GUCY1B3* (p.Val412 to p.Leu572) and two GTP molecules. The model was built with the YASARA 10.8.16 software package analogue to CCT7η. The average quality Z-score after validation with WHAT_CHECK was −1.2. A structure file of the models and the alignments are available on request (Supplementary Fig. 5A, B).

sGC and CCTη mutants, platelet homogenates and cGMP-forming activity. The *GUCY1A3* subunit of sGC and CCTη was cloned by standard procedures from a human fetal brain library sub-cloned into pcDNA3.1Zeo(+) (*GUCY1A3*; Invitrogen) or pCMV6 (*CCT7*, OriGene). The *GUCY1A3* construct was co-expressed with the bovine β1 subunit, which only exerts six amino acid differences compared to the human sequence. The respective mutations were introduced with the Quick Change site-directed mutagenesis kit from Stratagene and verified by sequencing. HEK 293 cells cultured in DMEM supplemented with 5% heat-inactivated FCS were seeded at 660,000 cells per flask (25 cm^2). The next day, cells were transfected with 2.6 μg cDNA of each of the sGC subunits with FuGENE6 transfection reagent (Roche Diagnostics) according to the manufacturer's instructions. After transfection (60–70 h), cells were collected, washed and resuspended in 400 μl ice-cold buffer (50 mM NaCl, 50 mM triethanolamine/HCl, pH 7.4, containing 2 mM D,L-dithiothreitol (DTT), 1 mM EDTA, mammalian protease inhibitor cocktail (Sigma-Aldrich)), lysed by sonification (one 5-s pulse) or by passing through a 27-gauge needle (10×). After centrifugation (800*g*, 10 min, 4 °C) to remove cell debris, the protein concentration was determined in the supernatant using the Bradford Protein Assay (Bio-Rad).

Human venous blood samples (20 ml) were immediately mixed with acid citrate dextrose (5 ml, 85 mM trisodium citrate, 70 mM citric acid, 110 mM glucose). After a first centrifugation (200*g*, 15 min, room temperature), the supernatant was collected and centrifuged (1,000*g*, 10 min, room temperature), and the resulting platelet-containing pellet was resuspended in 1 ml WP buffer (5 mM HEPES, pH 7.4, 150 mM NaCl, 0.55 mM NaH_2PO_4, 7 mM $NaHCO_3$, 2.7 mM KCl, 0.5 mM $MgCl_2$, 5.6 mM glucose). Subsequently, cells were lysed by sonification (one 5-s pulse) and samples were centrifuged (20,000*g*, 15 min, room temperature). The protein content was determined in the supernatant (platelet homogenate). Samples (10 μg) were analysed in western blot for the α1 and β1subunit of sGC with specific antibodies[5]. Quantification of the signals was performed by chemiluminescence detection with a CCD camera system.

For the determination of sGC activity, supernatants (10 μg HEK 293 cell or platelet homogenate, see above) were measured at different NO concentrations (0–10 μM GSNO HEK 293 cells, or 100 μM GSNO platelets) in the presence of 300 μM GTP, 3 mM $MgCl_2$, 3 mM DTT, and 50 mM triethanolamine/HCl, pH 7.4, in a total volume of 0.1 ml for 10 min at 37 °C. Subsequently, reactions were stopped and the formed cGMP was measured in a RIA as described in more detail previously[5].

CCT7 knockdown by siRNA. HASMC (GIBCO, C-007-5C) were cultured in smooth muscle cell media 2 (PromoCell). Cells were 50–70% confluent at time of transfection. Lipofectamine RNAiMAX reagent (Invitrogen) was used for transfection according to the manufacturer's instructions. In brief, three pooled *CCT7* siRNAs (Santa Cruz, sc-43449), equivalent to a final concentration of 10–20 nM, were incubated with RNAiMAX reagent in Opti-MEM medium without serum for 20 min at room temperature. Afterwards, RNAi—RNAiMAX complexes were added to the cell cultures and incubated for 40 h at 37 °C in a saturated humidity atmosphere containing 5% CO_2. In parallel, cells were transfected with 20 nM of scrambled RNA as control.

Lysis of the cells was performed in lysis buffer (50 mM HEPES, pH 7.5, 1 mM EDTA, 1% (v/v) Nonidet-P40 (NP 40), 0.5 mM LiCl, and proteinase inhibitor cocktail (Roche)). After the addition of SDS-loading buffer (62 mM Tris, pH 6.8, 2% (w/v) SDS, 10% (v/v) glycerol and 5% (v/v) 2-mercaptoethanol) 0.005% (w/v) protein solutions were separated by SDS–PAGE (10% bisacrylamide/acrylamide) and blotted onto PVDF (polyvinylidene difluoride) membranes (Roche). Anti-CCT7 (Sigma, HPA008425), anti-GUCY1A3 (ref. 5) and GUCY1B3 (ref. 5) antibodies were used for protein detection.

Total RNA was extracted from transfected cells using the RNA easy mini kit (Qiagen) according to manufacturer's instructions. RNA was reverse-transcribed into cDNA with the Super Script First-Strand Synthesis System III (Invitrogen). Expression levels of *CCT7*, *GUCY1A3* and *GUCY1B3* were measured by TaqMan analysis using appropriate probes from Life Technologies (*CCT7*, *Hs00362446_m1*; *GUCY1A3*, *Hs01015574_m1*; and *GUCY1B3*, *Hs00168336_m1*). *HPRT* and *YWHAZ* probes (Life Technologies) served as reference genes. All measurements were performed in duplicates per PCR run. At least three runs were carried out for each sample.

Thrombus formation *in vivo* in mice deficient for α1-sGC ($\alpha1^{-/-}$). The experiments conformed to the guide for the care and use of laboratory animals published by the US National Institutes of Health, were performed in accordance with the German Animal Welfare Act and approved by local authorities (Landwirtschafts- und Umweltministerium Schleswig-Holstein, V312-72241.122-2). Experiments were performed in 3–8-month-old male mice deficient in α1-sGC ($\alpha1^{-/-}$)[5] and respective wild-type animals in a similar genetic background (BL6). Mice were housed at the animal facility of the university with free access to water and food (standard diet, Altromin) under a 12-h light/12-h dark cycle at a room temperature of 20 °C with a maximum of six mice per cage. All surgery was performed

under anaesthesia. Initially, animals were anesthetized by an intraperitoneal injection of fentanyl (0.1 mg kg^{-1}), midazolam (2 mg kg^{-1}) and medetomidin (20 mg kg^{-1}), followed by continuous intravenous application via a catheter placed in the jugular vein. During further preparation and throughout the experiment, mice were regularly pinched in the paw with forceps and also shortly blown on their whiskers to test for reactions as well as level of consciousness, and the rate of anaesthesia infusion was accordingly adjusted. The animals were tracheotomized for artificial ventilation during the experiment and their body temperature was maintained at 37 °C by convective heat. The right cremaster muscle was prepared for intravital microscopy on a custom-made stage as described[22] and continuously superfused with warmed (34 °C) saline solution (in mmol l^{-1}: 143 Na^+, 5 K^+, 2.5 Ca^{2+}, 1.2 Mg^{2+}, 127 Cl^-, 25 HCO^{3-}, 1.2 SO_4^{2-} and 1.2 H_2PO^{4-}), gassed with 5% CO_2 and 95% N_2 ($pCO_2 \approx 40$ mm Hg, $pO_2 \approx 30$ mm Hg) at rate of 8 ml min^{-1}. Arterioles were observed using a microscope (Axioskop 2FS, Zeiss) equipped with a video camera (PCO, XC-77CE, Computer Optics). Images were displayed on a video monitor and recorded on videotape (Panasonic, AG-5700) for later measurement of platelet aggregation and the vessels luminal diameter after image digitization.

In all experiments, indometacin (3 μmol l^{-1}) was added to the superfusion to block prostaglandin production 30 min before the start and throughout the experiment. During this period, 10 arterioles with diameters ranging from 7 to 51 μm (21.7 ± 1.4 and 22.3 ± 1.6 μm in wild-type and $\alpha1^{-/-}$ mice, respectively; $P = 0.80$) were chosen in each animal according to visibility and size. For later photoexcitation, high molecular mass FITC-dextran (MW 150000, TdB Consultancy AB) was injected intravenously (5 μl of a 20% solution per gram body mass) and allowed to circulate for at least 10 min before the start of the experiment. Platelet aggregation was initiated by photoexcitation of the circulating dye at 450–490 nm using a mercury lamp (HBO 100, Zeiss) and appropriate filters (filter set 09, Zeiss) in a circle with a diameter of ~100 μm that contained the arteriole under study. If flow stoppage due to thrombus formation was observed in the arteriole, further excitation was interrupted. Time to visible aggregation (onset) and time to complete arteriolar closure identified by flow stop were assessed. Arterioles with flow cessation without observing a local occluding thrombus were excluded from analysis. After studying about half of the pre-chosen vessels consecutively in the presence of indometacin, the NO-synthase inhibitor L-NA (30 μmol l^{-1}) was also applied to the superfusion solution and the second half of the vessels studied in a similar fashion. Arterioles were allocated to treatment group according to size and location within the network. Hereby, vessels of comparable sizes were assigned to each group. To avoid the examination of an arteriole downstream in the network of a beforehand-studied vessel, the latter were examined first. In some experiments, L-NA and indometacin was applied from the start to balance observation numbers between treatment groups. Therefore, the examiner was aware of the treatment as well as of the genotype of the animal under study. At the end of the experiment, maximal arteriolar diameter was assessed during superfusion of a combination of different dilators (adenosine, SNP and acetylcholine, 30 μmol$^{1-1}$ each) before the animal was killed by injection of pentobarbital.

Association analysis. For the SNP rs7692387, located in intron 6 of the *GUCY1A3* gene, we performed a two-stage analysis: a meta-analysis of GWAS for discovery, and a replication stage in additional cohorts for confirmation. As discovery stage, we used data of 22,233 cases and 64,762 controls from CARDIoGRAM[23], a meta-analysis of 14 GWAS of CAD and MI, and combined these with replication data of an additional 6,500 cases and 10,266 controls from 5 additional studies (Angio-Lueb/KoraF3, PopGen, Luric/Emil, WTCCC-CAD2, and GerMIFS IV/BASE-II). A fixed effect, pooled model was used to estimate the effect size. Details of the design of CARDIoGRAM have been published previously[24]. Only subjects reporting European ancestry were included.

For both stages, we performed analyses in each study separately. Genotyping in all studies except GerMIFS IV was carried out on Affymetrix or Illumina platforms. In GerMIFS IV, SNP rs7692387 was genotyped with TaqMan. Quality control of data was performed centrally according to previously agreed criteria including quality of the imputation, deviation from Hardy–Weinberg equilibrium in the controls, and SNP call rate.

For the CARDIoGRAM studies, a log-additive model frequency test adjusting for age (onset of the first event for cases or time of recruitment for controls) and gender and taking into account the uncertainty of possibly imputed genotypes were performed. For Angio-Lueb/KoraF3, PopGen, Luric_Emil and WTCCC2, logistic regressions were performed adjusting for age (onset of the first event for cases or time of recruitment for controls) and gender. For GerMIFS IV, a chi-squared test was performed. A summary estimate was computed using a fixed-effect model weighting each study by the inverse of its variance. A level of association of $P < 5 \times 10^{-8}$ (Bonferroni correction for 1,000,000 independent SNPs) in the combined analysis of the discovery and replication samples was assumed as significant.

Study information. LUdwigshafen RIsk and Cardiovascular Health (LURIC) study: consists of angiographically confirmed CAD (at least one coronary vessel with a stenosis >50%) cases[25]. The controls included population-based non-case subjects, and were part of a control series (Echinococcus Multilocularis and Internal Diseases in Leutkirch study (EMIL)[26]) that consisted of healthy, unrelated blood donors recruited between May and July 2004 from the south-western area of Germany.

PopGen: PopGen consists of unrelated German patients with CAD recruited in Schleswig-Holstein, through the population-based PopGen biobank with significant CAD (at least a 70% stenosis in one major coronary vessel) and age of onset <55 years, the controls were population-based[27].

Angio-Lueb/KORA F3: Lübeck Registry of Structural Heart Disease[27] consist of consecutive patients referred for coronary angiography, classified as CAD or MI cases based on the coronary angiogram (at least a 50% stenosis in one major coronary vessel) and age of onset (<65 years in males, and <70 years in females). The Kooperative Gesundheitsforschung in der Region Augsburg (KORA) F3 consisted of population-based controls.

GerMIFS IV: cases consists of consecutive patients referred for coronary angiography, classified as CAD or MI cases based on the coronary angiogram (at least a 50% stenosis in one major coronary vessel) and age of onset (<65 years in males, and <70 years in females). Control samples were recruited as part of the Berlin Aging Study II (BASE-II), a multidisciplinary study investigating factors related to human ageing. All subjects were recruited from the Berlin metropolitan area and underwent an extensive phenotypic assessment, including a two-day medical examination. None of the BASE-II subjects included here reported a history of CAD or MI, nor showed any current signs of acute cardiovascular disease. This sample included a total of 1,105 individuals (424 women and 681 men, average age at examination 56.6 years (s.d. 16.5)).

Genotyping and imputation of BASE-II. After applying standard quality-control thresholds (per sample missing rate ≤ 5%, per SNP missing rate ≤ 2%, Hardy–Weinberg equilibrium $P > 1 \times 10^{-6}$), high-quality microarray-based genotypes (using the 'Genome-Wide Human SNP Array 6.0' (Affymetrix, Inc.)) were available for 710,205 autosomal SNPs across 1,125 BASE-II subjects. These were subjected to genome-wide SNP imputations via IMPUTE v2.026 (ref. 28) using precompiled 'HapMap 3 + 1000GP CEU+TSI' panels from the IMPUTE website (Dec 2010 release). These contain HapMap 3 data (from release #2, Feb 2009) and 1,000 Genomes Project data from Phase I (interim_ (based on a sequence freeze in Aug 2010, and haplotype phasing released in Dec 2010) for autosomal SNPs. IMPUTE's average posterior call info and certainty metrices for rs7692387 were 0.966 and 0.986, respectively. For the purpose of this study, genotypes for rs7692387 were hard-coded disregarding dosage data, if individual information and certainty scores were ≥ 0.9 ($n = 1{,}060$), or coded as missing, if one or both metrics fell below 0.9 ($n = 44$).

WTCCC-CAD2. The WTCCC-CAD2 cases ($n = 1{,}213$) comprised patients with a validated history of CAD (92.7% with MI; 19.3% females, mean age at diagnosis 53.5 ± 9.6 years). Controls are from the UK 1958 birth cohort (mean age at recruitment 44 years, 43.9% females). All cases and controls were of white Caucasian origin recruited in the United Kingdom. Further details on the cohorts and genotyping are provided in the Supplementary Information.

Statistical analysis. Means and proportions for clinical characteristics and risk factors at baseline were calculated for CAD and MI cases and controls. Student's *t*-test was used to evaluate differences in means for normally distributed data, otherwise the Wilcoxon and Mann–Whitney test were used. Several comparisons were corrected according to Bonferroni. The chi-squared statistic was used to compare proportions. Conditional logistic regression models were applied after matching for analysis time, age in decades, and gender. Relative risk estimates were obtained in addition to crude models adjusted for several cardiovascular risk factors, including systolic blood pressure, smoking, body mass index, diabetes mellitus, and plasma lipid levels. All *P*-values are two-tailed, and values of less than 0.05 were considered to indicate statistical significance. Confidence intervals were calculated at the 95% level.

All subjects in all studies gave written informed consent before participating. All studies were approved by their local ethics committees.

13. Broeckel, U. *et al.* A comprehensive linkage analysis for myocardial infarction and its related risk factors. *Nature Genet.* **30,** 210–214 (2002).
14. Fischer, M. *et al.* Distinct heritable patterns of angiographic coronary artery disease in families with myocardial infarction. *Circulation* **111,** 855–862 (2005).
15. Adzhubei, I. A. *et al.* A method and server for predicting damaging missense mutations. *Nature Methods* **7,** 248–249 (2010).
16. Risch, N. Linkage strategies for genetically complex traits. III. The effect of marker polymorphism on analysis of affected relative pairs. *Am. J. Hum. Genet.* **46,** 242–253 (1990).
17. Dekker, C. *et al.* The crystal structure of yeast CCT reveals intrinsic asymmetry of eukaryotic cytosolic chaperonins. *EMBO J.* **30,** 3078–3090 (2011).

18. Krieger, E. *et al.* Improving physical realism, stereochemistry, and side-chain accuracy in homology modeling: Four approaches that performed well in CASP8. *Proteins* **77,** 114–122 (2009).
19. Krieger, E., Darden, T., Nabuurs, S. B., Finkelstein, A. & Vriend, G. Making optimal use of empirical energy functions: force-field parameterization in crystal space. *Proteins* **57,** 678–683 (2004).
20. Krieger, E., Nielsen, J. E., Spronk, C. A. & Vriend, G. Fast empirical pK_a prediction by Ewald summation. *J. Mol. Graph. Model.* **25,** 481–486 (2006).
21. Liu, Y., Ruoho, A. E., Rao, V. D. & Hurley, J. H. Catalytic mechanism of the adenylyl and guanylyl cyclases: modeling and mutational analysis. *Proc. Natl Acad. Sci. USA* **94,** 13414–13419 (1997).
22. Wölfle, S. E., Schmidt, V. J., Hoyer, J., Kohler, R. & de Wit, C. Prominent role of $K_{Ca}3.1$ in endothelium-derived hyperpolarizing factor-type dilations and conducted responses in the microcirculation *in vivo*. *Cardiovasc. Res.* **82,** 476–483 (2009).
23. Schunkert, H. *et al.* Large-scale association analysis identifies 13 new susceptibility loci for coronary artery disease. *Nature Genet.* **43,** 333–338 (2011).
24. Preuss, U. W., Koller, G., Zill, P., Bondy, B. & Soyka, M. Alcoholism-related phenotypes and genetic variants of the CB1 receptor. *Eur. Arch. Psychiatry Clin. Neurosci.* **253,** 275–280 (2003).
25. Ritsch, A. *et al.* Cholesteryl ester transfer protein and mortality in patients undergoing coronary angiography: the Ludwigshafen Risk and Cardiovascular Health study. *Circulation* **121,** 366–374 (2010).
26. Haenle, M. M. *et al.* Overweight, physical activity, tobacco and alcohol consumption in a cross-sectional random sample of German adults. *BMC Public Health* **6,** 233 (2006).
27. Schunkert, H. *et al.* Repeated replication and a prospective meta-analysis of the association between chromosome 9p21.3 and coronary artery disease. *Circulation* **117,** 1675–1684 (2008).
28. Marchini, J., Howie, B., Myers, S., McVean, G. & Donnelly, P. A new multipoint method for genome-wide association studies by imputation of genotypes. *Nature Genet.* **39,** 906–913 (2007).